ISPRS Journal of Photogrammetry and Remote Sensing 64 (2009) 1–16

Contents lists available at ScienceDirect

ISPRS Journal of Photogrammetry and Remote Sensing

journal homepage: www.elsevier.com/locate/isprsjprs

Full-waveform topographic lidar: State-of-the-art

Clément Mallet *, Frédéric Bretar

Laboratoire MATIS - Institut Géographique National, 2-4 Avenue Pasteur 94165 Saint-Mandé Cedex, France

ARTICLE INFO

Article history:
Received 15 May 2007
Received in revised form
12 September 2008
Accepted 12 September 2008
Available online 29 October 2008

Keywords:
Lidar systems
Full-waveform data
Literature survey
Waveform analysis
Signal processing

ABSTRACT

Airborne laser scanning (ALS) is an active remote sensing technique providing range data as 3D point clouds. This paper aims at presenting a survey of the literature related to such techniques, with emphasis on the new sensors called full-waveform lidar systems. Indeed, an emitted laser pulse interacts with complex natural and man-made objects leading to a temporal distortion of the returned energy profile. The new technology of full-waveform laser scanning systems permits one to digitize the complete waveform of each backscattered pulse. Full-waveform lidar data give more control to an end user in the interpretation process of the physical measurement and provide additional information about the structure and the physical backscattering characteristics of the illuminated surfaces. In this paper, the theoretical principles of full-waveform airborne laser scanning are first described. Afterwards, a review of the main sensors as well as signal processing techniques are presented. We then discuss the interpretation of full-waveform measures with special interest on vegetated and urban areas.

Contents

* Corresponding author. Tel.: +33 1 43 98 80 00x7566; fax: +33 1 43 98 85 81.
E-mail addresses: clement.mallet@ign.fr (C. Mallet), frederic.bretar@ign.fr (F. Bretar).
URLs: http://recherche.ign.fr/labos/matis (C. Mallet), http://recherche.ign.fr/labos/matis (F. Bretar).

0924-2716/$ – see front matter
doi:10.1016/j.isprsjprs.2008.09.007

1. Introduction

Airborne laser scanning (ALS) is an active remote sensing technique providing direct range measurements between the laser scanner and the Earth's topography. Such distance measurements are mapped into 3D point clouds. The altimetric accuracy of a topographic lidar measurement is high (<0.1 m). Depending on the geometry of illuminated surfaces, several backscattered echoes can be recorded for a single pulse emission. This is particularly interesting in forested areas, since lidar systems can measure both the canopy height and the terrain elevation underneath at once, contrary to photogrammetric techniques. Moreover, lidar data are known to be useful in many specific applications such as 3D city modeling, bridge and power line detection or Digital Terrain Model generation.

Airborne lidar data only give a basic geometric representation of a scene. Consequently, many authors have developed new automatic mapping algorithms for point classification (Filin, 2002; Sithole, 2005), urban reconstruction (Haala and Brenner, 1999; Rottensteiner and Briese, 2002) and forest assessment (Hyyppä et al., 2004). Most of them are only based on the point cloud geometry and sometimes on the intensity (Hug and Wehr, 1997).

Since 2004, new ALS commercial systems called **full-waveform** lidar have appeared with the ability to record the complete waveform of the backscattered signal echo. Thus, in addition to range measurements, further physical properties of objects included in the diffraction cone[1] may be derived with an analysis of the backscattered waveforms.

This article presents a state-of-the-art on full-waveform lidar systems as well as related processing techniques. First, we describe the physical principles of lidar systems as well as the theoretical contribution of full-waveform lidar. The second part of the article is a taxonomy of both bathymetric, experimental, and commercial full-waveform systems. We especially focus on the first main systems, developed by NASA and carried by satellite platforms. Then, full-waveform data processing methods are presented. Studies on the relationship between geometric and radiometric surface parameters and pulse shapes are discussed. Eventually, we conclude with a detailed description of full-waveform lidar data applications both on forested areas – including parameter estimation and modeling – and urban areas.

[1] The term "diffraction cone" will be used in this article in preference to "laser footprint". We would like to emphasis the fact that the laser beam reaches several objects at different heights whereas the term "laser footprint" is when the beam reaches the ground (2D consideration).

2. Topographic laser scanning systems

2.1. Presentation of airborne and spatial systems

2.1.1. Introduction

A topographic lidar device is a laser rangefinder delivering a reliable, accurate but irregular representation of terrestrial landscapes through georeferenced 3D point clouds (Baltsavias, 1999b). The first active sensors carried by airborne or satellite platforms were designed at the beginning of the 1970s. They provided 1D profiles along the sensor track (nadir view) by sequences of single pulses. Modern sensors acquire many parallel strips of 150–600 m swath width, which may overlap, due to a specific scan pattern. Such technology provides denser point clouds with a more regular distribution on the Earth's surface: the point density can reach more than 100 pts/m^2 in some specific applications, *e.g.*, river dike monitoring.

Topographic lidar is now fully operational for many specific applications such as metrology (Fidera et al., 2004), forest parameters estimation (Andersen et al., 2005), target or power line detection (Sithole and Vosselman, 2006), corridor, coastal (Irish and Lillycrop, 1999) or opencast mapping.

2.1.2. Physical principles

Both pulsed and continuous wave lasers are being used. Pulsed systems measure the round-trip time of a short light pulse from the laser to the target and back to the receiver. Continuous wave systems carry out ranging by measuring the phase difference between the transmitted and received signal. This state-of-the-art focuses on pulsed systems.

ALS physical principle consists in the emission of laser pulses from an airborne platform at a high repetition frequency (PRF). The two-way runtime of the backscattered signal from the sensor to the Earth surface is measured: it enables range estimation from the lidar system to the landscape (Baltsavias, 1999b).

Depending on the wavelength, the emitted electromagnetic wave interacts with atmospheric particles (absorption or scattering, known to have negligible influence if rain is excluded), but mainly with illuminated natural or man-made objects belonging to the Earth surface.

The PRF depends on the acquisition mode (see part 2.2.3) and on the flying altitude. A pulse release is done when the previous pulse recording is effective (even if, in fact, the PRF is constant). However, the latest systems have even the ability to fire a second laser pulse before the recording of the previous pulse (Roth and Thompson, 2008).

3D point cloud is obtained by direct georeferencing processes: a system using both GPS (differential measurements with a ground

station located near the survey area) and inertial measurements (IMU) is used to optimally calculate supporting vector attitudes and the absolute orientation of the laser sensor (Heipke et al., 2002).

Basic airborne lidar systems consist of a laser transmitter and a receiver (rangefinder unit which receives the reflected pulses and measures the distance), a mechanical scanner, a hybrid positioning system, a storage media, and an operating system for signal digitization and on-line data acquisition. This unit monitors and synchronizes measurements, and processes data in real-time to extract georeferenced points (Baltsavias, 1999a; Thiel and Wehr, 2004).

2.1.3. Lidar measurement formulas

The standard lidar equation is derived from the radar equation. It describes the measurement process by taking the detector and target characteristics into account. It also relates the power of transmitted and return signals (Jelalian, 1992). More explicit formulas have been proposed to model real world constraints (Der et al., 1997; Carlsson et al., 2001). Nevertheless, they are only valid for single sources or for flat surfaces. In case of targets that are distributed in space, the reflected signal is the superposition of echoes at different distances.

It can be expressed as an integral:

$$P_r(t) = \frac{D^2}{4\pi\ \lambda^2} \int_0^H \frac{\eta_{\text{sys}}\ \eta_{\text{atm}}}{R^4} P_t\left(t - \frac{2R}{v_g}\right) \sigma(R)\mathrm{d}R \tag{1}$$

where t is the time, D the aperture diameter of the receiver optics, P_r the received power, P_t the emitted power, λ the wavelength, H the flying height, R the distance from the system to the target, η_{atm} and η_{sys} respectively the atmospheric and system transmission factors, v_g the group velocity of the laser pulse, and $\sigma(R)\mathrm{d}R$ the apparent effective differential cross-section (Wagner et al., 2006). The cross-section is called "apparent" since an object reflecting the signal at a given distance can occlude an object further away.

The power of the received signal can also be considered as the sum of the contribution of N targets with their own characteristics:

$$P_r(t) = \sum_{i=1}^{N} P_{r,i}(t) * \eta_{\text{sys}}(t) * \eta_{\text{atm}}(t) \tag{2}$$

where $P_{r,i}(t)$ is the echo of the ith object expressed as:

$$P_{r,i}(t) = \frac{D^2}{4\pi\ \lambda^2} \int_{R_i-\Delta R}^{R_i+\Delta R} \frac{1}{R^4} P_t\left(t - \frac{2R}{v_g}\right) \sigma_i(R)\mathrm{d}R \tag{3}$$

where R_i is the mean distance, $[R_i - \Delta R, R_i + \Delta R]$ the spatial spread and $\sigma_i(R)$ the effective differential backscattering cross-section. The reflected signal can be seen as the convolution between the transmitted pulse and the effective differential cross-section. As a consequence, when $\Delta R \ll R$, we have:

$$P_{r,i}(t) \approx \frac{D^2}{4\pi\ \lambda^2\ R_i^4} P_t(t) * \sigma_i'(t) \tag{4}$$

where $\sigma_i'(t)$ is the apparent cross-section of illuminated areas within each range interval. The power of the received signal can finally be expressed as:

$$P_r(t) = \sum_{i=1}^{N} \frac{D^2}{4\pi\ \lambda^2\ R_i^4} \underbrace{P_t(t) * \eta_{\text{sys}}(t)}_{\text{system contribution}} * \underbrace{\eta_{\text{atm}}(t) * \sigma_i'(t)}_{\text{environment contribution}} . \tag{5}$$

2.2. Topographic lidar technology

2.2.1. Multiple pulse systems

The first commercially available airborne laser scanners provided only one backscattered echo per emitted pulse. The recording of a single echo is sufficient if there is only one target within the diffraction cone. However, even for small laser footprints (0.2–2 m), there may be many objects within the travel path of the laser pulse: individual scattering contributions are generated for each encountered object. **Multi-echo** or **multiple pulse** laser scanning systems are designed to record more than one echo. They typically collect first and last pulses. Some are able to discriminate up to six individual returns from a single pulse (Thiel and Wehr, 2004). The two first echoes contain about 90% of the total reflected signal power. Real-time detection of more than five pulses requires thus the detection of low intensity signal within noise.

Fig. 1 shows a comparison between first pulse and last pulse in a urban area. Two Digital Elevation Models have been generated from first pulse and last pulse point clouds. Thus, the height difference has been computed. Multiple reflections occur on vegetated areas. When the vegetation is not very dense, it is often assumed that the first echo belongs to the canopy top and the last pulse to the ground. In reality this is not always the case. It can only be checked with 3D display tools. In a particular viewing angle, when the laser beam hits a building edge, two echoes can be generated. The first pulse corresponds to the roof while the second one to the ground.

2.2.2. Geometric quality of laser scanning

Laser altimetry is a technique known to provide elevation data with reliability and high altimetric accuracy (<0.1 m) as well as a good planimetric accuracy (<0.4 cm) even under forested areas (Ahokas et al., 2003). Compared with multi-stereo high-resolution photogrammetric products, lidar points are certainly more accurate but less dense. Irregular spatial sampling is one of the main problem, as the density of points rarely exceeds 25 pts/m^2 for particular applications. The lack of information from commercial firms on real-time 3D point calculation methods makes it difficult to know the local measurement errors within the point clouds. Nevertheless, many errors alter the range measurement. Among the general error budget, systematic errors can be calibrated (bias in measuring the mirror angle, hardware problems in synchronizing and integrating measurements, incorrect point detection during real-time analysis, GPS/IMU co-ordinations etc) whereas random ones cannot (IMU temporal drift, variations in the signal to noise ratio of the return signal, electronics accuracy and surface reflectivity variations within the diffraction spot).

The errors on lidar measurements have been studied in detail by many authors (Schenk, 2001). A more detailed description of determining the position of the aircraft can be found in Bretar (2006) whereas Huising and Pereira (1998) list the main sources of errors in the laser measurement for various detectors.

2.2.3. Pulse detection methods

For multi-echo systems, pulse detection is performed in real-time on the backscattered signal. The hardware system detector turns a continuous waveform to several time-stamped pulses, giving the position of individual targets. Many peak detection methods exist, but lidar manufacturers do not provide any information about the method implemented in their hardware systems. The number and the timing of the recorded pulses are critically dependent on the detection method (Wagner et al., 2004; Jutzi and Stilla, 2005a). Fig. 2 presents an example of wrong pulse detection with the threshold method. An erroneous detection (*e.g.*, weak echoes missed) could lead to a misinterpretation of the

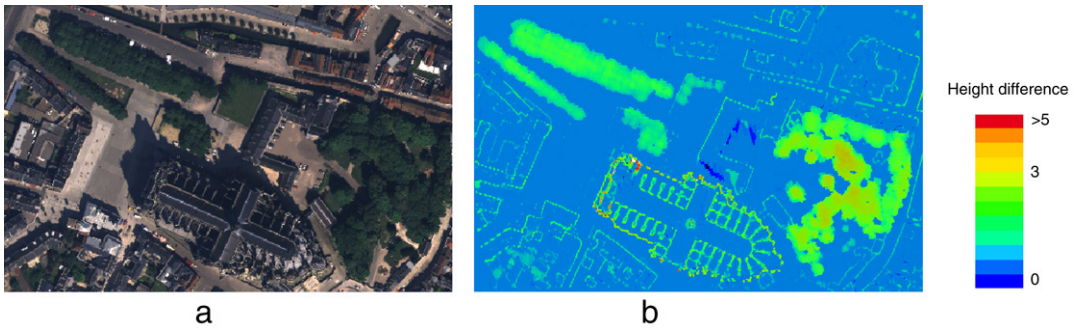

Fig. 1. First pulse and last pulse height comparison. Vegetated areas and building edges are clearly visible. (a) Orthophotography on the city of Amiens, France (0.25 m resolution ©IGN). (b) Difference between first and last pulse Digital Elevation Models.

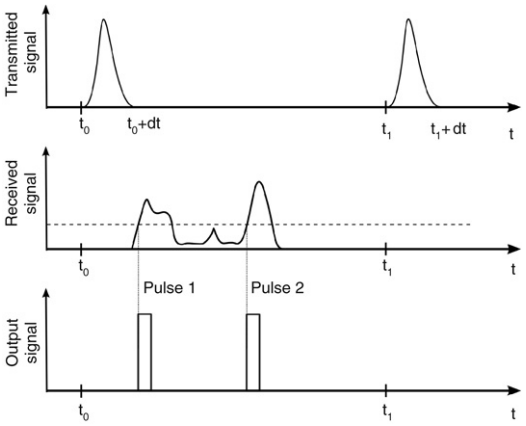

Fig. 2. Simplified pulse emission (*above*) and the corresponding received signal (*middle*). Two significant peaks are detected with the threshold method (*middle and bottom*). Two echoes will be generated for this pulse instead of four.

survey area, whereas a shift between the real-time detected pulse position and the real location leads to an inaccurate position of the object (more than 0.3 m in some cases). Moreover, in presence of low ground vegetation in woodlands or street items in urban areas, the detection method would not be able to find two echoes if the range between two targets is less than 1.5 m. Lidar waveform processing permits to cope with most of these issues.

2.2.4. The advent of full-waveform lidar systems

Waveform analysis allows one to set up advanced processing methods which increase pulse detection reliability, accuracy and resolution. Furthermore, the new technology of full-waveform lidar systems gives more control to the end user in the interpretation process of the physical measurement. It provides additional information about the structure and the physical backscattering properties of the illuminated surface (reflectance and geometry).

The first truly operational topographic system, LVIS (see Section 3.2 for more details) appeared in 1999 and demonstrated the value of recording the entire waveform for vegetation analysis (Blair et al., 1999). The first commercial full-waveform lidar system appeared in 2004 (Hug et al., 2004). Section 3 gives a comprehensive list of the names, manufacturers and characteristics of such laser scanning systems.

Full-waveform systems sample the backscattered waveform at a frequency of around 1 GHz. They allow one to determine the vertical distribution of targets hit by a laser pulse.

The understanding of such waveforms requires a pre-processing step. On the one hand, waveforms can be decomposed into a sum of echoes to generate a 3D point cloud (Section 4). Resulting data can then be used in classical lidar algorithms (classification, building reconstruction, etc.). On the other hand, new approaches are also conceivable. They are based on the captured waveforms using a "1D signal topology" instead of a 3D point cloud (*cf.* part 6.2).

2.2.5. Recording full-waveform data

To record the waveform, *i.e.* the laser backscattered energy as a function of time, lidar manufacturers have added digitization terminals to their systems and hard disks with high storage capacity. The waveforms are usually digitized on 8 bits. The volume of data is bound to be five times superior to the 3D point cloud over the same area. The main limitation of surveying areas with a full-waveform lidar system is subsequently the storage capacity. For example, the Optech ALTM 3100 device is able to collect data during 3 h and 20 min with a 300 GB hard drive, with a PRF equal to 50 kHz.

The two main techniques for recording the signals are described in Jutzi and Stilla (2003).

Whatever the lidar system method, the constant digitization sampling period varies between 1 and 10 ns. The waveform is not integrally recorded but only for a predefined maximum number of samples. Indeed, it is necessary to avoid massive storage problems. For example, Optech ALTM systems can store up to 440 samples for each pulse. This is equivalent to a discrete vertical section of 66 m (440×0.15 m per sample). The TopEye MarkII system saves 128 samples according to a predefined mode which is either "*first pulse and later*" (127 samples after the first) or "*last pulse and earlier*". It means that full-waveform systems will not record, within a given waveform, both echoes from the canopy and from the ground, if the trees are taller than the maximum "recording length" of the system.

The present issue with full-waveform data deals with data handling and management since much larger data volume are now recorded.

3. Typology of full-waveform lidar systems

The first full-waveform systems were designed in the 1980s for bathymetric purposes (Guenther and Mesick, 1988). Topographic devices appeared in the mid-1990s with experimental systems and have been commercially available for a few years. Full-waveform topographic lidar systems mainly differ in footprint size, pulse energy and PRF. Small-footprint and large-footprint systems do not collect the same information over the same area. The applications therefore differ from a system to another.

Most commercial systems are small-footprint (0.2–3 m diameter, depending on flying height and beam divergence) with higher PRF. They provide a high point density and an accurate altimetric description within the diffraction cone (Fig. 3(a)). Nevertheless, mapping large areas requires extensive surveys. Besides, small-footprint systems often miss tree tops. It is difficult to

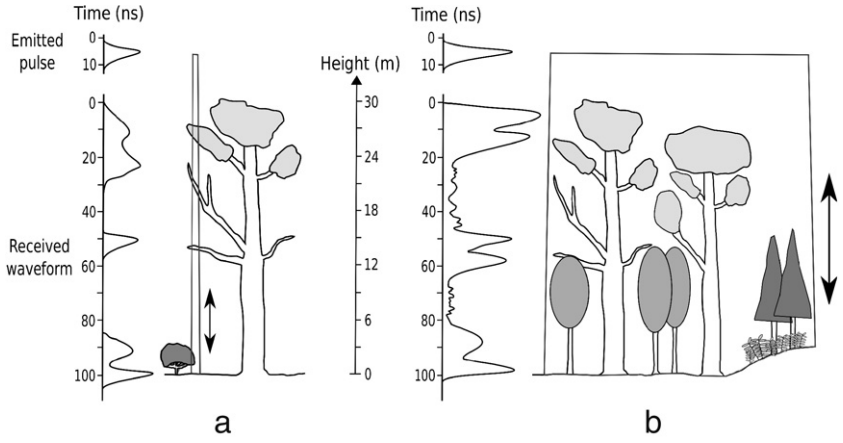

Fig. 3. Transmitted and received signals in a wooded area with (a) a small-footprint lidar and (b) a large-footprint lidar. With a small-sized footprint, all targets strongly contribute to the waveform shape but the laser beam has a high probability of missing the ground. When considering large footprints, the last pulse is bound to be the ground but each echo is the integration of several targets at different locations and with different properties.

determine whether the ground has been reached under dense vegetation. Consequently, ground and tree heights cannot be well estimated (Dubayah and Blair, 2000).

Large-footprint systems (10–70 m diameter) increase the probability to both hit the ground and the canopy top. They avoid the biases of small-footprint systems. Thus, the return waveform gives a record of the vertical distribution of intercepted surface within a wider area (Fig. 3(b)). The first experimental full-waveform topographic systems were large-footprint and mostly carried by satellite platforms. With a higher flying height, pulses must be fired at a lower frequency and with a higher energy.

3.1. Bathymetric lidar systems

Designed for accurate sea-depth determination, they are composed of two beams, one green (532 nm) and one infrared (1064 nm). The green beam traverses the air-water interface and propagates in the water until the sea bottom with the least attenuation. The infrared beam is reflected by the water and gives the range from the plane to the sea surface. Bathymetric waveforms are therefore composed of two peaks. Processing these waveforms consists of finding the two main signal maxima and deriving the range values. We will not go into further detail regarding bathymetric lidar systems in this article. More information is available in Guenther et al. (2000).

There are currently several bathymetric lidar systems: **LARSEN-500**, the very first bathymetric system, **LADS** (Laser Airborne Depth Sounder), the **SHOALS** series (Scanning Hydrographic Operational Airborne Lidar Survey), fully operational since 1994, **Hawk Eye**, developed in Sweden on a model similar to SHOALS and **EAARL** (Experimental Advanced Airborne Research Lidar), developed by NASA in 2002. Their main characteristics are described in Section 3.4.

3.2. Experimental lidar systems

The following prototypes developed by NASA have been designed to assess the characteristics of woodlands or land cover. They aim at mapping large areas to provide data at a resolution of several meters and a swath width up to 1–2 km.

- *Scanning Lidar Imager of Canopies by Echo Recovery (SLICER)*: the precursor of the topographic systems described below was designed to characterize the vertical structure of the canopy. This medium-sized footprint airborne device demonstrated that full-waveform systems could be used to assess the characteristics of woodlands, distinguish tree ages and species, and characterize the structure of extensive areas (Lefsky et al., 1999b). SLICER data can be downloaded on line (SLICER, 2008).
- *Shuttle Laser Altimeter (SLA)*: this satellite sensor was designed to cover seas, clouds, and land (glaciology, tectonics, hydrology, geomorphology, etc.). Two versions were produced, SLA-01 and 02 (1996–1997), for a feasibility study for the future MBLA and GLAS systems. SLA-02 was used to verify the accuracy of a global 1 km resolution DTM and thus characterize some systematic biases (Harding et al., 1999).
- *Laser Vegetation Imaging Sensor (LVIS)*: this improved version of SLICER was used to test and provide data for developing algorithms, calibrating instruments and evaluating the performance of measurements to assess the future Vegetation Canopy Lidar (VCL) mission (*cf.* MBLA system). It also demonstrated the potential of full-waveform data to characterize woodland areas and measure the Earth's topography, even below the canopy (Blair et al., 1999). It was mainly used to develop a real-time algorithm for classifying ground points by analyzing the return waveform. Sample data from this system are public (LVIS, 2008).
- *Multi-Beam Laser Altimeter (MBLA)*: the MBLA system was part of the VCL mission (Vegetation Canopy Lidar). VCL is an active space-based lidar remote sensing system consisting of a five beam instrument with 25 m contiguous along track resolution. VCL aimed at providing data sets for understanding major environmental issues (climatic change, sustainable land use), and improving global biomass and carbon stocks estimation. VCL's core measurement objectives were canopy top heights, vertical distribution of intercepted surfaces and ground surface topographic elevations (VCL, 2008). This programme was due to be launched in 2003 but was abandoned.
- *Geoscience Laser Altimeter System (GLAS)*: the five year ICESat satellite mission, carrying GLAS sensor, was launched in January 2003 to study the evolution of land and sea glacial masses in the Antarctic and Greenland, the roughness and thickness of sea ice, the topography (using a 1064 nm laser) and the vertical structure of clouds and aerosols (532 nm laser) (Geophysical Research Letters, 2005; GLAS, 2008). ICESat classifies the return waveform in real-time into land/ice and icesheet/sea by analyzing the return waveform and recognizing Gaussian distributions from which the main characteristics are extracted (Brenner et al., 2003). Data sets are available on the mission Web site (ICESat, 2008).

3.3. Commercial lidar systems

Operational versions of commercial full-waveform systems have been available since 2004. These small footprint systems have considerable potential but do not have any dedicated application (Hug et al., 2004). The manufacturing companies are Riegl (Austria), Toposys (Germany), TopEye/Blom (Sweden) and Optech (Canada). Leica (Switzerland-Germany) ALS-series do not currently have a full-waveform digitizer but are working on it.

3.4. Technical specifications of the main existing systems

Tables 1 and 2 summarize the main characteristics of the full-waveform lidar systems mentioned above.

Notes:

- *Final year*: blank if the system is still in use.
- *Wavelength*: when two wavelengths are given (typically 1064 and 532 nm), this means that the system includes two lidar systems, each with its own wavelength. These are either bathymetric applications or satellites with dual coverage (land and sea).
- From *Flying height* to *Range accuracy*: the characteristics are given as ranges of values. These are manufacturer's data and are limited by the system's flying height. The formulas for determining the exact values for a given height can be found in Baltsavias (1999b).
- *Range accuracy*: this is the accuracy given by the manufacturers after on-line peak detection in the return waveform (telemeter accuracy). It is distinct from the along-track minimum distance between two consecutive peaks and from the altimetric accuracy of lidar data.
- In a cell, "-" means that the information is unknown or not available.

4. Processing the backscattered waveform

4.1. Existing approaches

Two approaches are conceivable for processing the vertical profiles recorded by the new generation of airborne lidar sensors. On one hand, it consists of decomposing the waveform into a sum of components or echoes, so as to characterize the different targets along the path of the laser beam. The aim of this approach is to maximize the detection rate of relevant peaks, to generate a denser 3D point cloud and, finally, to extend waveform processing capabilities by fostering information extraction from the raw signal. Increasing the number of 3D points is of interest for forestry applications (*cf.* Section 6.1.1). Extracting more information can be useful for segmentation and classification purposes, in both forested and urban areas (see Section 5).

On the other hand, the whole 1D signal is preserved. A spatio-temporal analysis is applied to find features within a 3D waveform space. This approach is suitable for urban areas where the geometry is regular (*cf.* Section 6.2).

The latter approach has been barely investigated. Most research on full-waveform analysis has been focused on the enhanced 3D point cloud. This section therefore deals with waveform decomposition. If advanced techniques are efficient to extract strong and weak echoes and for range determination (Section 4.2), other approaches model the waveforms using analytical functions (Section 4.3).

4.2. Range determination and echo extraction

4.2.1. A deconvolution approach for range determination and target discrimination

Based on a physical understanding of the pulse propagation and its interaction with the illuminated surface, Jutzi and Stilla (2006) propose a relevant algorithm to discriminate different surface responses which are very closely located in range (<0.15 m).

First, the received waveform of the backscattered pulse is computed using the lidar equation (formula (5)). It depends on the transmitted waveform (modeled by a Gaussian function randomly modulated by a Gaussian noise), on the spatial energy distribution of the emitted pulse (also modeled, depending on the laser device), on the surface response (with given reflectance and geometric properties, here with two differently elevated specular plan plates), on the atmospheric transmission, and receiver efficiency. Then, the waveform is processed in four main steps:

- pulse detection with a noise dependent threshold;
- deconvolution in the Fourier domain of the transmitted waveform with the received waveform;
- estimation of the surface function using the Wiener Filter; the Wiener Filter is a real function estimated from the modulated transmitted waveform and the background noise;
- waveform fitting with the Levenberg–Marquardt technique using the surface function as modeling function (see part 4.3.2).

Finally, experiments on different kinds of surfaces show that surfaces with a distance corresponding to less than 0.15 m can be resolved.

4.2.2. Advanced echo extraction methods

The main reason for decomposing the waveform is to extract more points in a more reliable way. Several methods have been carried out so far. They are described in this section. Waveform fitting algorithms, described in Section 4.3.2, also permit to find peak location and echoes undetected by traditional pulse detection methods. However, they require to model the echoes with an analytical function. But an inappropriate model can lead to erroneous results.

- *Detection of weak pulses*. Stilla et al. (2007) show it is possible to detect weak pulses corresponding to partially occluded targets or objects with poor surface backscatter properties. A waveform stacking technique is performed by establishing neighborhood relationships between consecutive waveforms. Mutual information is therefore accumulated to produce a "global" scattering for such targets. This technique predicts new pulses not detected by standard algorithms.
- *Improved range determination*. For urban landscapes, Kirchhof et al. (2008) propose a method to improve the point density, the range accuracy as well as the segmentation between partially penetrable objects and impenetrable surfaces. The goal of this approach is to fill gaps that can appear in partly occluded surface regions. Assuming that the laser beam hits a planar surface with a given slope, the surface response is modeled (transmitted and received waveforms are known) using a matched filter. It produces range values and generates a 3D point cloud. Points are segmented according to a given feature and those expected to belong to impenetrable surfaces are used to estimate surface primitives. A new surface response is finally computed and used as prior knowledge at the beginning of the algorithm.

  This method (as well as the deconvolution approach) allows one to determine the range of each echo without any pulse shape assumption and to detect weak echoes corresponding to partially occluded and partly illuminated regions.

Table 1
Main technical specifications for full-waveform lidar systems.

System	Company manufacturer	Platform	Beam deflection	Beginning–final year	Wavelength (nm)	Flying height (km)	Pulse rate (kHz)
Bathymetric							
LARSEN 500	Terra Surveys Optech	Airborne	Rotating mirror	1983–	1064/532	0.5	0.02
MarkII	LADS TopEye	Airborne	Fibers	1989–	1064/532	0.37–0.5	0.9
Hawk Eye	Saab Optech	Airborne	Oscillating mirror	1990–	1064/532	0.05–0.8	0.2
SHOALS 1000T	US army Optech	Airborne	Oscillating mirror	1994–	1064/532	0.2–0.4	0.4
EAARL	NASA	Airborne	Oscillating mirror	2002–	1064/532	0.3	3
Experimental							
SLICER	NASA	Airborne	Oscillating mirror	1994–1997	1064	<8	0.075
SLA-02	NASA	Satellite	None	1996–1997	1064	285	0.01
LVIS	NASA	Airborne	Oscillating mirror	1997–	1064	<10	0.1–0.5
GLAS	NASA	Satellite	None	2003–	1064/532	600	0.04
MBLA	NASA/University of Maryland	Satellite	Oscillating mirror	None	1064	400	0.01/0.242
Commercial							
LMS Q560	Riegl	Airborne	Polygon	2004–	1550	<1.5	≤100
Falcon III	TopoSys	Airborne	Fibers	2005 –	1560	<2.5	50–125
MarkII	TopEye	Airborne	Palmer	2004–	1064	<1	≤50
ALTM 3100	Optech	Airborne	Oscillating mirror	2004–	1064	≤3.5	≤70
ALS60	Leica	Airborne	Oscillating mirror	2006–	1064	0.2–6	≤50

Table 2
Main technical specifications for full-waveform lidar systems (*second part*).

System	Pulse energy (mJ)	Pulse width (ns)	Scan rate (Hz)	Scan angle (°)	Beam divergence (mrad)	Footprint size (m)	Range accuracy (cm)	Digitizer (ns)
LARSEN 500	–	12	20	30	4	2@500 m	30	1
LADS MarkII	7	–	18	27	–	–	15	2
Hawk Eye	2/15	7	0.3–7	0/40	2–15	1–7.5@500 m	30	1
SHOALS 1000T	2/15	6	0.3–7	0/40	2–15	0.8–6@400 m	15	1
EAARL	0.07	1.3	25	22	0.03	0.15@300 m	3	1
SLICER	–	4	80	–	2	10@5 km	11	1.35
SLA-02	40	8	–	–	0.3	85@285 km	150	4
LVIS	5	10	500	14	8	40@5 km	30	2
GLAS	75/35	6	–	0	0.11–0.17	66@600 km	5–20	1
MBLA	10	5	–	–	0.06	24@400 km	100	4
LMS Q560	0.008	4	5–160	45	0.5	0.5@1 km	2	1
Falcon III	–	5	165–415	28	0.7	0.7@1 km	–	–
MarkII	–	4	<50	14/20	1	1@1 km	2–3	1
ALTM 3100	<0.2	8	<70	50	0.3/0.8	0.3/0.8@1 km	1	1
ALS60	<0.2	5	<90	75 usually	0.22	0.22@1 km	2	1

4.3. Modeling and fitting the waveforms

When modeling the echoes within a waveform, a parametric approach is always chosen. Parameters of a mathematical model are estimated for each detected peak in the signal. These parameters provide additional information about the target characteristics (shape and reflectance) and extend waveform processing capabilities. Statistical elements extracted by signal processing techniques are the number of significant peaks, their range to the sensor and the parameters of the modeling function. A single function is always used to model all echoes of the waveforms.

One wishes to decompose a waveform $y = f(x_i)$ into a sum of n components:

$$y_i = \sum_{k=1}^{n} \phi_k(x_i) + b_i \tag{6}$$

where f is the waveform model, ϕ the echo model with a set of parameters $\boldsymbol{\theta}$ ($f = \sum_k \phi_k$), $\{x_i\}_{i=1,\ldots,N}$ is a sequence of uniformly-spaced points, $y = \{y_i\}_{i=1,\ldots,N}$ the sampled waveform, and b the noise.

A relevant echo model is particularly suitable so that related parameters should be used for segmenting the 3D point cloud. A large body of literature addresses the issue of fitting waveforms with a given parametric model.

4.3.1. Modeling the waveforms

A waveform is a convolution between a laser transmitted pulse (assumed to be of Gaussian shape with a calibrated width) and a "surface" scattering function, often considered as a Gaussian function (Wagner et al., 2006). The received signal is then assumed to be a mixture of Gaussian distributions. Such modeling is the most frequently used to process full-waveform data. The analytical expression of the Gaussian function is:

$$\phi_k(x) = A_k \exp\left(-\frac{(x-\mu_k)^2}{2\sigma_k^2}\right) \tag{7}$$

where A_k is the pulse amplitude, σ_k the pulse width, μ_k the pulse range. Thus, $\boldsymbol{\theta}_k = \{A_k, \sigma_k, \mu_k\}$.

The Gaussian model is sufficient for most applications, especially for large-footprint lidar data (Zwally et al., 2002; Wagner et al., 2006). However, for small-sized and medium-sized footprints, this model is not always justified. In urban areas, many

peaks are distorted: indeed, most of the return waveforms are subject to the mixed effects of geometric (*e.g.*, roof slopes) and radiometric object properties (*e.g.*, different kinds of street and roof materials). Hence, the characteristics of return peaks may differ significantly. Consequently, other modeling functions have been proposed in Chauve et al. (2007). For instance, it has been shown that the generalized Gaussian function, which is an extension of the Gaussian function, improves signal fitting and models distorted peaks.

4.3.2. Fitting the waveforms

Several methods have been carried out to fit the waveform with a single modeling function:

- Non-linear least-squares approach using Levenberg–Marquardt optimization algorithm,
- Maximum likelihood estimate with *Expectation–Maximization* algorithm,
- Stochastic approach using Reversible Jump Monte Carlo Markov Chain method.

► *Non-linear least-squares approach*. Hofton et al. (2000) give a description of a non-linear least-squares method which is used in bathymetric (Wong and Antoniou, 1991), satellite (Brenner et al., 2003), terrestrial (Jutzi and Stilla, 2006) and airborne laser scanning systems (Duong et al., 2008; Reitberger et al., 2008a).

This problem is a system of N observations with $m \times n$ unknown parameters. $m = \text{card}\,\boldsymbol{\theta}$ is the number of parameters of the modeling function and n the number of echoes. The quality of the results is evaluated by a variable ξ. One aim at fitting the data with a prescribed accuracy ϵ.

$$\xi = \sqrt{C \sum_{i=1}^{N} (f(x_i) - y_i)^2} < \epsilon \tag{8}$$

where C is a weight: $C = 1/N$ in Hofton et al. (2000) or $C = 1/(N - \text{card}\,\boldsymbol{\theta})$ in Chauve et al. (2007).

The system is solved using a non-linear least-squares method, the Levenberg–Marquardt (LM) technique (Marquardt, 1969). An iterative algorithm is used. There is no algorithm for solving the problem directly since the $\{\phi_k\}_k$ are not linear functions. The LM algorithm is known to be robust but requires a good initialization step.

Initial values are mainly provided by traditional pulse detection methods (Wagner et al., 2006). Besides, raw waveforms are noisy and are sometimes smoothed. The intensities above a threshold are considered to be potential echoes. Moreover, to overcome the problem of a wrong initialization step, Hofton et al. (2000) add progressively peaks in the least-squares fitting algorithm according to their amplitude until ξ is greater than a given threshold. Chauve et al. (2007) propose an iterative approach: after coarse peak detection, missing peaks are found in the difference between the modeled and the initial signals. If new peaks are detected, the fit is performed again. This process is repeated until no further improvement is possible.

► *Maximum likelihood approach: the EM algorithm*. Persson et al. (2005) have developed a pulse detection method based on the Expectation–Maximization algorithm (EM) (Dempster et al., 1977). The EM algorithm is a two-stage iterative optimization technique for finding maximum likelihood solutions. EM alternates between performing an expectation (E) step, which computes an expectation of the likelihood, and a maximization (M) step, which computes the maximum likelihood estimates of the parameters by maximizing the expected likelihood found on the E step. It consists in computing, for each sample, the probability of belonging to one of the kth distributions which decomposes the signal. Parameters found during the M step are then used to begin another E step, and the process is repeated. This method is a general technique. They assume that the return waveform is a sum of Gaussians. Nevertheless, it is possible to choose other probability density functions to fit the return waveforms.

► *Reversible Jump Monte Carlo Markov Chain method*. Levenberg–Marquardt and Expectation–Maximization algorithms require the explicit gradient expression of the modeling function. This is a drawback for complex analytical functions: the first derivative for all parameters is not always computable. Moreover, it has already been shown that the more parameters to be estimated, the more inconsistent fitting results appear (Chauve et al., 2007). Hernández-Marín et al. (2007) have proposed a method to fit terrestrial lidar waveforms with a specific modeling function (a set of four piecewise exponential functions), that can be adapted to geospatial topographic waveforms. For that purpose, the Reversible Jump Monte Carlo Markov Chain (RJMCMC) method is used. A grammar of functions can be defined and this optimization algorithm will find the best model. It can even find the best mixture of functions with the optimal parameters (Green, 1995). The fitting algorithm is based on the formulation of an energy, allowing the introduction of prior knowledge related to the object layout (*e.g.*, surface reflectance) and to the waveform decomposition (the number of echoes can be limited). Consequently, a signal fitting algorithm using the RJMCMC technique is relevant: it is robust (the global minimum of the energy is found), no initialization and no gradient are required, and the grammar of models is extensible.

4.4. Conclusions

The literature shows that the main process applied to lidar profiles is signal decomposition and modeling. The advantages of waveform processing is threefold. First, the different algorithms presented in the previous sections no longer limit the number of peaks that can be detected. Additional points are therefore extracted. As expected, it concerns those with low intensity, located where multiple echoes appear, or overlapping echoes (*cf.* Fig. 4 and all papers cited in this section). Such points are not recorded by a conventional multiple pulse system due to internal thresholds for peak detection. Consequently, on forested areas, waveform processing can for instance provide up to 60% more pulses than real-time system (Reitberger et al., 2008a; Chauve et al., in press). This result depends on the tree species, the leaf-on/leaf-off conditions and the survey specifications. Figs. 5 and 6 show on a profile and on different tree species additional points that can be extracted. In urban areas, new peaks are found in the tree canopy as well as on building edges. When the laser beam hits an edge, a low amplitude pulse corresponding to the ground can appear after the roof echo.

Second, waveform processing improves object range determination, even over complex surfaces (Zwally et al., 2002). For instance, in forested areas, both canopy and ground height estimates can be improved (Duong et al., 2008) but this result depends on the survey specifications and the landscape (Chauve et al., in press). In urban areas, range accuracy of solid opaque targets can also be bettered (Kirchhof et al., 2008). Consequently, the modeling of the landscape is improved: the processing of Digital Terrain and Digital Surfaces Model from point clouds take advantage of the better height determination.

Third, modeling the echoes provide additional parameters that can be useful for classification purposes (see Section 5).

The Gaussian approximation is shown to be satisfactory and sufficient for most of mapping applications in urban and

Fig. 4. Improvement of lidar waveform peak detection. (a) Waveform with two overlapping pulses: three pulses are detected with two overlapping ones. (b) Waveform with low intensity pulse: three pulses are detected with two of low amplitudes. In both signals, only one echo is found by hardware processing (vertical line). The crosses indicate the pulse location with post-processing.

Fig. 5. Comparison over a vegetated area between full-waveform lidar points and multiple pulse lidar points.

Fig. 6. Extracted points on different tree species from full-waveform data post-processing. (a) Deciduous (leaf-on). (b) Deciduous (leaf-off). (c) Coniferous. Red, green and blue points correspond respectively to the first, last and intermediate extracted pulses (Reitberger et al., 2008a).

vegetated areas, both for large-footprint and small-footprint lidar data (Hofton et al., 2000; Wagner et al., 2006). Wagner et al. (2006) show that fitting Gaussians to the echoes is however less satisfactory for high amplitudes. Furthermore, for low amplitude pulses, the estimation of the echo parameters is less accurate. Other models, such as the generalized Gaussian function, may be of interest.

5. Quantitative analysis of return waveforms

The signal processing step fits echoes with appropriate modeling functions: their parameters contain significant information on the roughness, slope and reflectivity of the hit surfaces. For segmentation and classification purposes, many studies have already been carried out to evaluate the effect of the transmission and reflection parameters of the signal on the shape of the waveforms. They are described below. Studies of the laser system calibration and intensity correction are also presented.

5.1. Behavior of a reflected waveform

Many elements which could modify the shape of the waveform have been studied so far by many authors:

Distance to the sensor and emission angle: Vandapel et al. (2004) test different distance and angle configurations with a terrestrial sensor. At short distances from the target, the peak is asymmetrical, with a long rise and a short trail. It becomes symmetrical as the distance increases. Variations in the shape are also noticed with changes in the angle of incidence. The smaller the angle, the narrower and more symmetrical the peak.

Roughness: different responses are noticed between smooth surfaces (one or two echoes if there are discontinuities) and porous surfaces (multiple echoes at different depths, equivalent to the behavior of trees and vegetation) (Vandapel et al., 2004).